

IMAGING OF THE DIAPHRAGM Mi-Young Jeung MD, Afshin Gangi MD PHD, Stephane Guth MD, Horia Marin MD, Françoise Hannequin MD, Dominique Charneau MD, Catherine Roy MD

Radiology B, University Hospital of Strasbourg, Strasbourg, France

1) summary

Numerous pathologic conditions may affect the diaphragm. Precise localization and characterization of these lesions may at times be difficult due to the shape and complex anatomic relationships of the diaphragm. Chest radiography is a useful screening tool for diaphragmatic abnormalities. Cross-sectional imaging including ultrasound, spiral CT with multiplanar reformation images, magnetic resonance imaging (MRI) can depict intrinsic pathology of the diaphragm and can assist in the evaluation of peridiaphragmatic masses by depicting the underlying complex anatomic relationship. Fluoroscopy is a useful additional study to evaluate the diaphragmatic motion, although ultrasound and MRI also are capable of this function. Knowledge of normal anatomy and various pathologic condition of the diaphragm and selection of the most appropriate imaging technique can greatly facilitate the diagnosis of diaphragmatic abnormalities.

2) Introduction

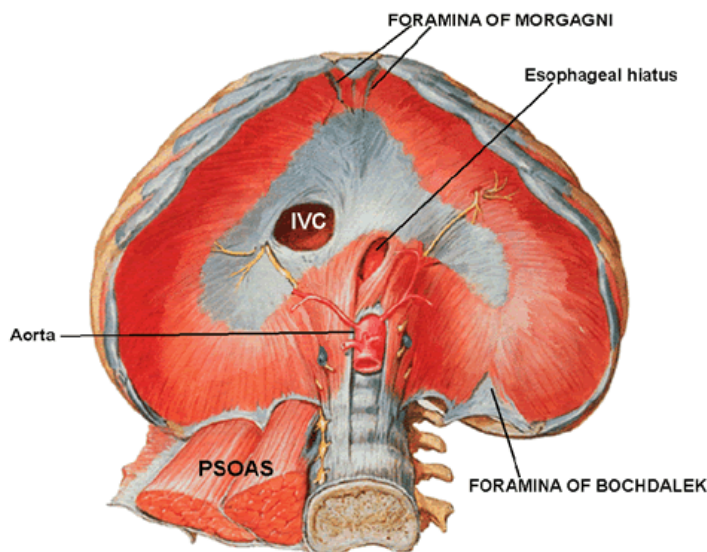
Diaphragm is a thin structure separating the thoracic and abdominal cavities. Numerous pathologic conditions may occur in and around the diaphragm. Due to the shape and complex anatomic relationships of the diaphragm, precise localization, and characterization of these lesions may be at times difficult. The aim of this exhibit is to review the normal diaphragmatic anatomy and its variants, and to illustrate imaging features of a variety of pathologies affect the diaphragm. Various imaging modalities will be presented, including plain radiography, ultrasonography, spiral CT with multiplanar

reformation and MR imaging with cine-mode. We will develop the guidelines for imaging choice to do a coherent and efficient work-up.

3) Anatomy

The diaphragm is a major muscle of ventilation and consists of a musculotendinous sheet separating the thorax and abdomen. Based on the origin of its muscle fibers, the diaphragm is divided into anterior or sternocostal part and a posterior or lumbar part, which may be functionally different. The muscle fibers from all parts insert into the boomerang-shaped central tendon. Three major openings in the normal diaphragm allow passage of the aorta, esophagus, inferior vena cava, and accompanying nerves and vascular and lymphatic channels. In addition to these normal openings, there are two symmetric "weak areas" known as the foramina of Morgagni and Bochdalek. The former is located anteriorly and the latter posterolaterally. They are sometimes the sites of diaphragmatic hernia.

ANATOMY OF THE NORMAL DIAPHRAGM VIEWED FROM BELOW



4) Normal appearance

Chest radiographs show the superior margin of each diaphragm as a dome-shaped interface between aerated lung and the opaque soft tissues of the abdomen. Pneumoperitoneum may reveal the thickness of the diaphragm by intraperitoneal free air silhouetting the inferior margin of the diaphragm (Fig 1). Variations in diaphragmatic contour such as scalloping and prominence of the costophrenic muscle slips are fairly frequent. On CT, the diaphragm can be visualized as a separate thin line structure only when its outer aspect is surrounded by the air in the lungs, or extraperitoneal fat, and its

inner aspect is margined by intraperitoneal or retroperitoneal fat (Fig 2). The plane of CT scan is not well suited to identifying the domes of the diaphragm, although this can be accomplished by using spiral CT and multiplanar reformations. On MR imaging, the diaphragm has the signal intensity similar to that of skeletal muscle, liver and spleen on all pulse sequences. The diaphragm is usually well visualized when it is surrounded by high signal-intensity abdominal or mediastinal fat. Given the superior contrast resolution and capability of direct multiplanar imaging, MR may prove of value in the assessment of diaphragmatic and peridiaphragmatic disease.

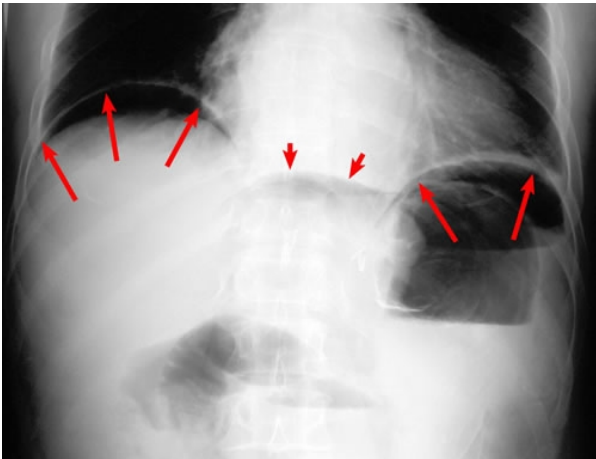
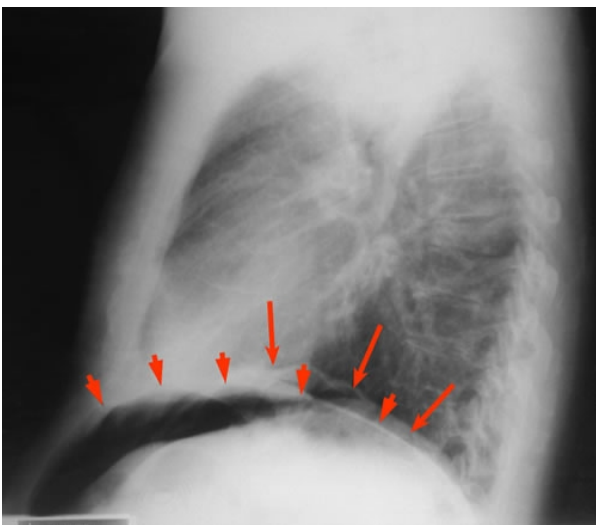


Fig 1: NORMAL DIAPHRAGM.



A. Posteroanterior radiograph shows well the shape and thickness of the diaphragm (big arrows) in a patient with a large pneumoperitoneum due to sigmoid perforation. Central anterior part of the diaphragm (small arrows) is also silhouetted by the air. B. Lateral radiograph: The right diaphragm (small arrows) is visible to the anterior chest wall. The left diaphragm (big arrows) is obscured anteriorly by the heart.

5) Normal variants

Occasionally, air within the most medial and inferior portions of the lower lobes, in apparent isolation from the remainder of the lung, can be seen on CT. This normal variant has been described by Silverman et al. as "retrocrural air" (Fig 1). This finding is visible in about 1 % of normal subjects. The shortened and thickened diaphragmatic muscle fibers near the costal insertion may indent the liver in a nodular or linear fashion (Fig 2). Nodularity of the diaphragm is accentuated on CT scan obtained in deep inspiration. Nodular infoldings of the diaphragm separate from the liver or spleen may mimic intrahepatic lesions or peritoneal tumor implants. The crura may simulate an enlarged lymph node on a single transaxial section on CT scan (Fig 3). Caskey et al. have suggested that many of the diaphragmatic defects identified, especially posteriorly in older patients, represent acquired defects occurring in areas of structural weakness, perhaps themselves embryologic in origin (Fig 4).



Fig 1: Retrocrural air (arrow).

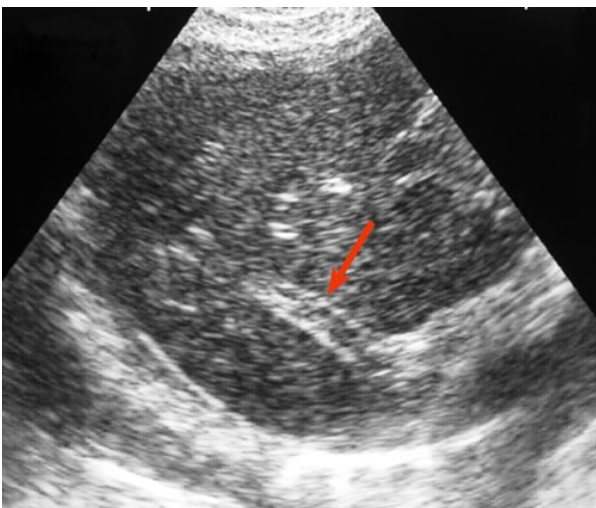


Fig 2: Ultrasound image: linear indentation of the diaphragm in the liver.

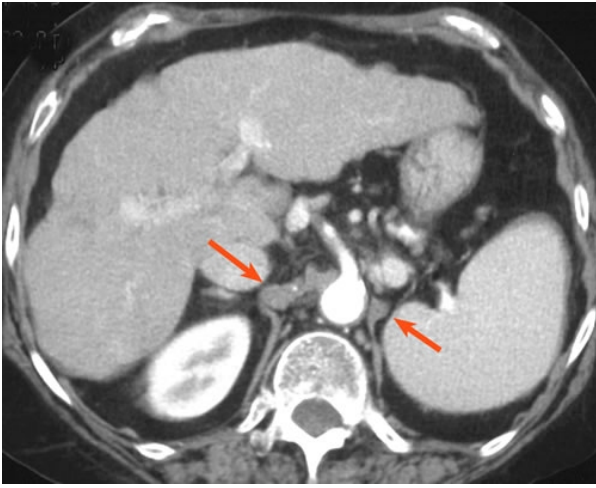


Fig 3: Nodular appearance of the crura: it should not be mistaken for adenopathy (arrow).

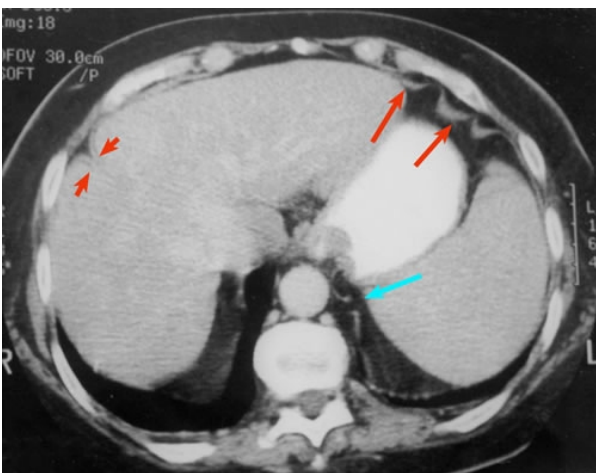


Fig 4: Indentation of the surface of the liver by the costal slip (arrowheads), diaphragmatic defect (curved arrow) and nodular folds (arrows).

6) Abnormal position or motion

- Eventration
- paralysis of the diaphragm
- restriction of motion

Eventration

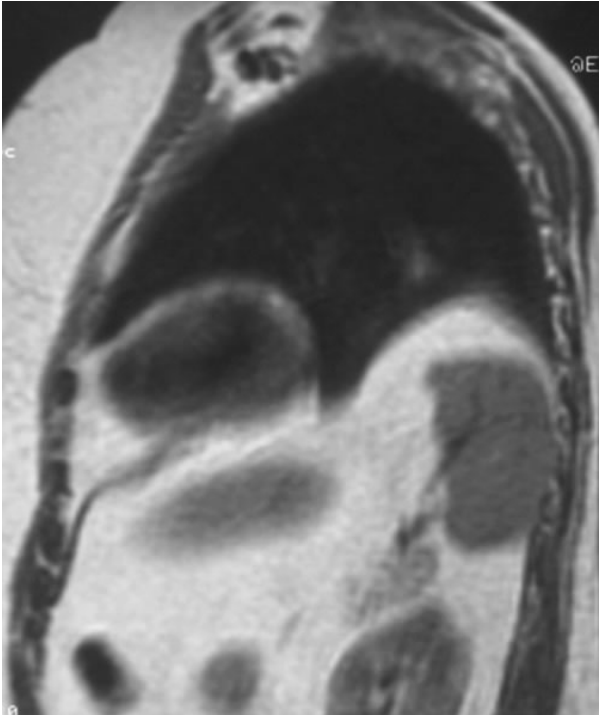
Eventration is a condition where all or a portion of hemidiaphragm is permanently elevated yet retains its continuity and normal attachments to the costal margins. It is a congenital anomaly due to the failure of muscular development of one portion or entire part of the diaphragm. Eventration occurs more often in males than in females. This most commonly presents in childhood on the right side, whereas in adults more often on the left side.

Partial eventrations usually manifest themselves as smooth, convex mounds interrupting the gentle curvature of the diaphragm normally seen on chest radiographs or MRI (Fig 1). Complete eventration shows the smooth elevation of the hemidiaphragm on radiographs, with slight paradoxical or little movement during inspiration on fluoroscopy and may be difficult or impossible to distinguish from diaphragmatic paralysis (Fig 2). CT, MR imaging, ultrasonography can be used to determine the contents of the eventration.

Fig 1: PARTIAL EVENTRATION



A. Posteroanterior and B. lateral radiographs in a 54-year-old woman demonstrate a broad, smooth bulging of anterolateral segment of the left diaphragm.



C. Coronal and D. sagittal T1-weighted MRI in a 65-year-old man shows a upward bulging of the posterior segment of the left diaphragm.

Fig 2: COMPLETE EVENTRATION.



Coronal T1-weighted MRI in a 57-year-old man shows an upward bulging of the entire right diaphragm. Dynamic MR imaging shows a slight paradoxal movement during a sniff.

Paralysis of the diaphragm

Diaphragmatic paralysis usually results from the interruption of nerve impulse transmission through the phrenic nerve. It may be unilateral or bilateral. The most common cause is the phrenic nerve invasion by a neoplasm, usually of pulmonary origin, although many cases are idiopathic. In these idiopathic cases, the paralysis is almost invariably right-sided and usually occurs in males. Traumatic injury of phrenic nerve can occur after radical neck or cardiothoracic surgery (stretch, section, or hypothermia), cervical manipulation, and cervical venipuncture. Patients with unilateral diaphragmatic paralysis are usually asymptomatic, although some patients may complain of dyspnea on effort. A paralyzed hemidiaphragm shows an elevated and accentuated dome configuration in both posteroanterior and lateral projection of chest radiographs (Fig 1). If the paralysis is left-sided, the stomach and splenic flexure of the colon relate to the inferior surface of the elevated hemidiaphragm

and usually contain more gas than normal. The sniff test on fluoroscopy is considered the most reliable way to detect diaphragmatic paralysis. The sniff test is accomplished by having the patient inhales rapidly and forcefully through the nose with the mouth closed. Normally both hemidiaphragms descend sharply during a sniff (Fig 2). Paradoxical upward motion of an entire hemidiaphragm, as seen in oblique or lateral projection, of greater than 2 cm is considered to diaphragmatic paralysis. Recruitment of abdominal expiratory muscles can cause a false-negative test. Definitive diagnosis of phrenic nerve paralysis can be obtained by cervical phrenic nerve stimulation with electromyographic measurement.

Fig 1: PARALYSIS OF THE DIAPHRAGM DUE TO TRAUMATIC INJURY OF PHRENIC NERVE (CONTUSION OF SCALENUS ANTERIOR)



Suspicion of diaphragmatic rupture in a 45-year-old man with motor vehicle accident 2 days earlier. Fig 1a. Chest radiograph: elevation of right hemidiaphragm and segmental atelectasis in the lower lobe. CT scan of the thorax shows no abnormality of the right diaphragm.

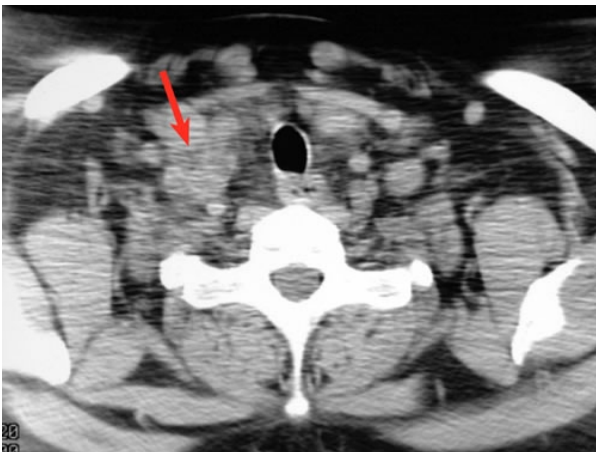



Fig 1b. CT section at the lower cervical level: multiple ill-defined low-density area in the enlarged right scalnus anterior (arrow), medius, and posterior muscles corresponding to contusion.

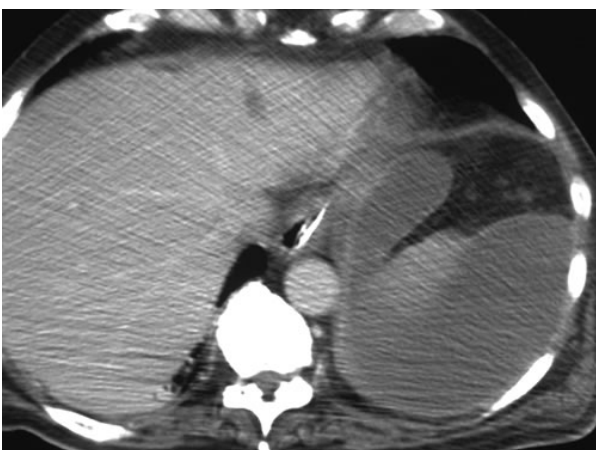
Fig 2. NORMAL DIAPHRAGMATIC MOVEMENT DURING A SNIFF.

Video shows a sharp descent of the diaphragm during a rapid inspiration in a 50-year-old healthy woman See in Movies : diaph.snif.n.02.mpg 

Restriction of diaphragmatic motion

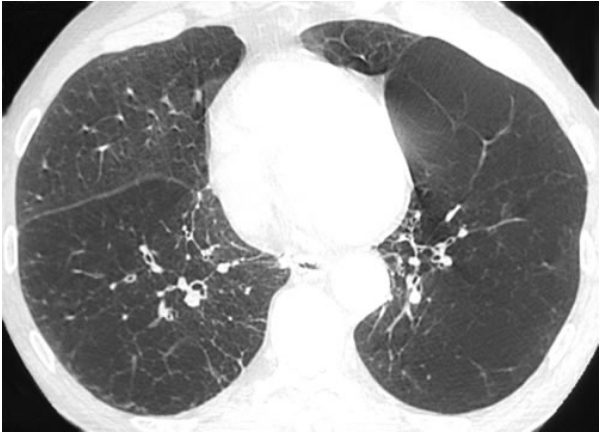
Diaphragmatic motion may be diminished due to acute inflammatory processes such as pneumonia, pleural effusion and subphrenic abscess (Fig 1) or in debilitated patients. Impaired inspiratory excursion of the diaphragm and rib cage due to a pain can produce the diaphragmatic elevation. The severe pulmonary hyperinflation due to chronic obstructive pulmonary disease or asthma prevent normal ascent of the diaphragm during expiration (Fig 2,3).

Fig 1: SUBPHRENIC ABSCESS



A 52-year-old man with septic shock 6 days after left hemicolectomy for colon cancer. A. portable chest radiograph: elevation of the left diaphragm with focal consolidation in the left lung base. B. CT scan: fluid collection in the left subphrenic area displacing the spleen.

Fig 2: ASYMMETRIC BULLOUS EMPHYSEMA



A 62-year-old man with exertional dyspnea. A. Chest radiograph: large bulla in the left lower lobe with compression of the adjacent parenchyma and left diaphragm. B. HRCT: massive destruction of the parenchyma by bullous emphysema involving more severely the left side. C. Dynamic MR imaging: inversion and inhibition of the ascent of the anterior portion of the left diaphragm during expiration.

Fig 3: SEVERE EMPHYSEMA

A 56-year-old man with previous history of lung reduction surgery in the left side 3 years ago. Dynamic MR imaging shows a flattening of the diaphragm and diminution of upward excursion of the diaphragm during expiration due to pulmonary overinflation.

See in Movies : [pirilot.emphyseme1.mpg](#)



7) Diaphragmatic hernias

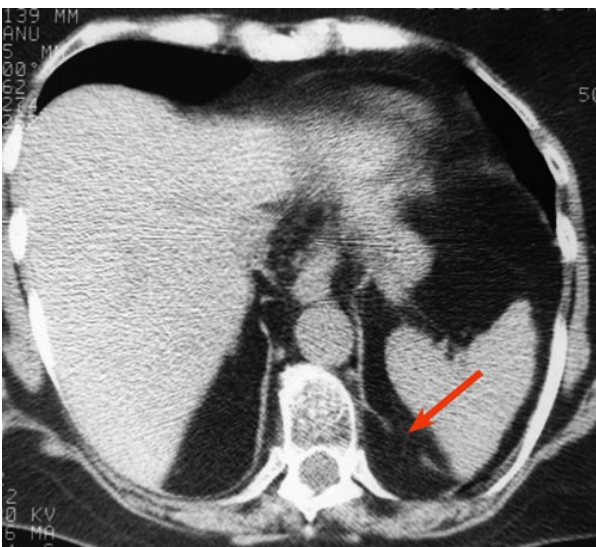
- bochdalek hernia
- Morgagni Hernia
- hiatal hernia
- traumatic hernia

bochdalek hernia

Bochdalek hernia is the most common form of diaphragmatic hernia. Gale reported an incidence of 6 per cent in 940 adults who had chest and abdominal CT examinations. Bochdalek hernia may occur if there is delayed or incomplete closure of the embryonic pleuroperitoneal membrane during the seventh week of gestation. These hernias are seen far more commonly on the left than on the right. The size of defect varies widely. A small defect may contain only retroperitoneal fat, a portion of the spleen or kidney, or omentum. When large, almost the entire abdominal contents may be in the hemithorax. Large Bochdalek hernias are a rare cause of severe acute respiratory distress in neonates

needing urgent surgical correction. The initial chest radiograph reveals the fluid-filled loops of bowel presenting as a water density cystic mass within the hemithorax, with varying degree of contralateral mediastinal shift. In the adult, Bochdalek hernia can present as a soft tissue mass adjacent to the posteromedial aspect of a hemidiaphragm on the chest radiography. CT scans or MR imaging can easily demonstrate the diaphragmatic defect and the hernia contents (Fig 1). Occasionally, spiral CT with sagittal or coronal reformation may be required to demonstrate small diaphragmatic defects (Fig 2). Hypogenetic lung syndrome may have associated anomaly such as Bochdalek hernia involving the right hemidiaphragm (Fig 3).

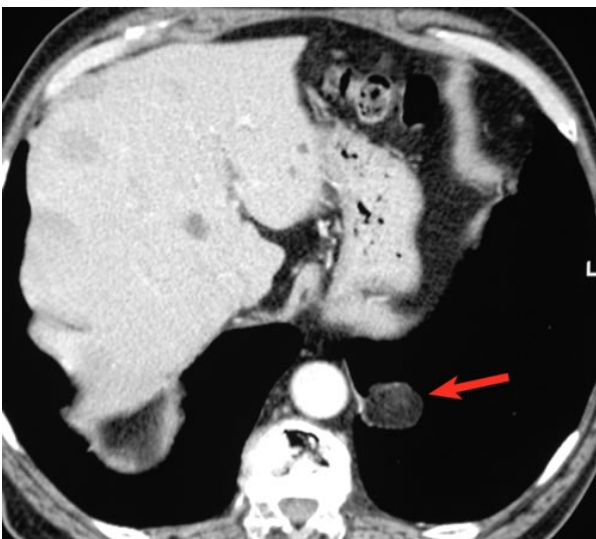
Fig 1: BOCHDALEK HERNIA

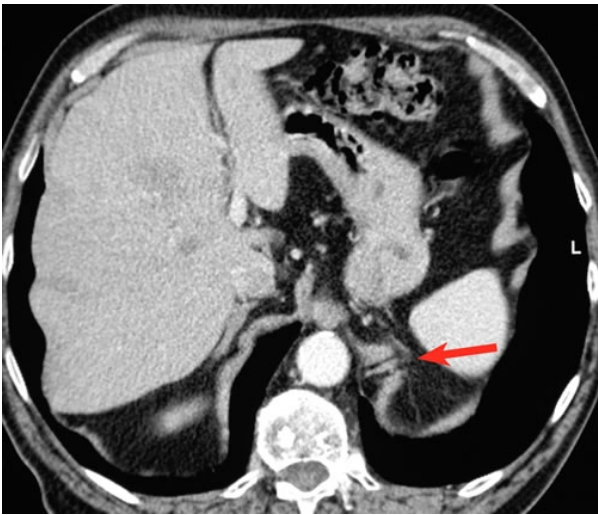




A 64-year-old asymptomatic woman. A. Routine chest radiograph: round regular mass in the retrocardiac area. B. CT scan: Small defect of the left diaphragm (arrow). C. Coronal T1-weighted MRI: herniated retroperitoneal fat through the diaphragmatic defect.

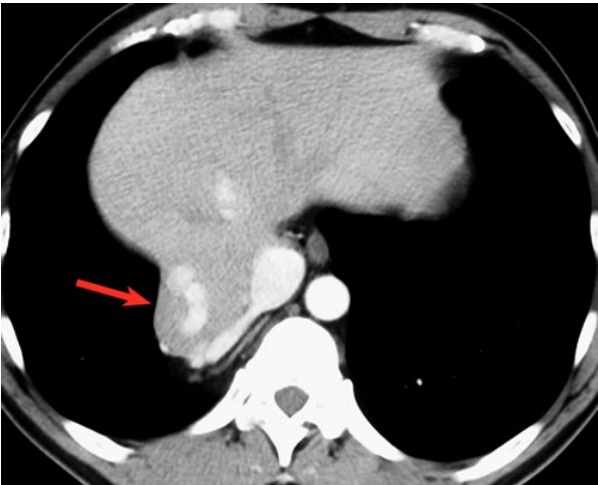
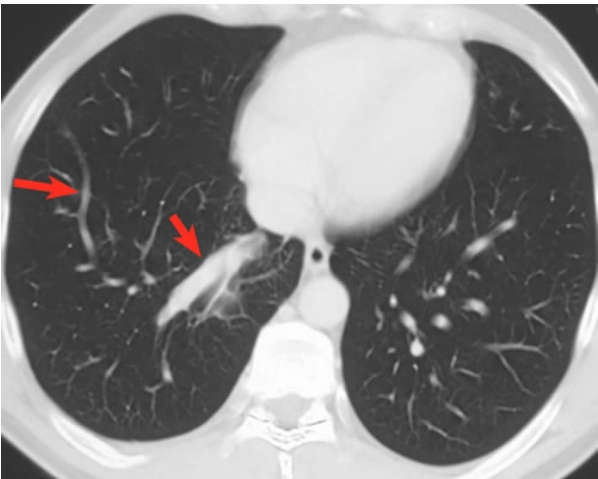
Fig 2: SMALL BOCHDALEK HERNIA

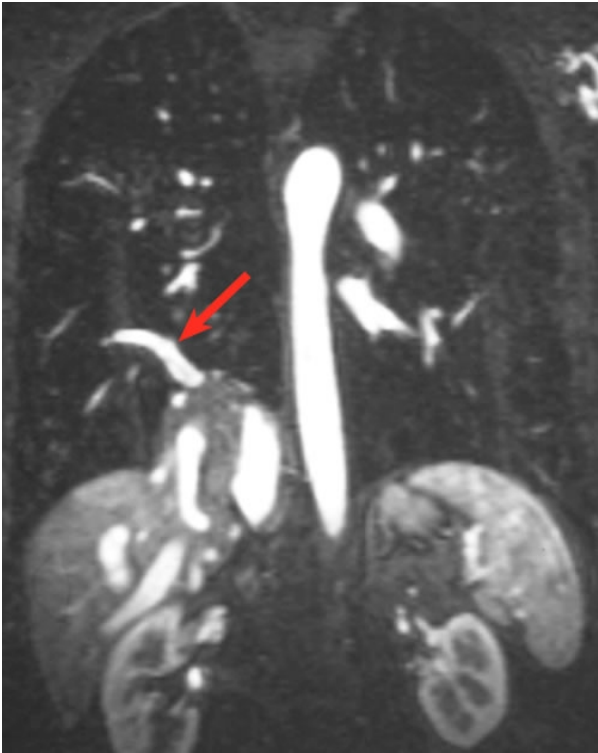




Follow-up CT scan after chemotherapy for bronchogenic carcinoma of the right upper lobe in a 68-year-old man. A. contrast-enhanced CT scan: fat-containing small nodule in the left lower lobe completely surrounded by pulmonary parenchyma, initially mistaken for metastasis at the pulmonary window setting. Also note hepatic metastases. B. CT scan at the lower level: small discontinuity in the left diaphragm. C. CT scan with sagittal reformation: mushrooming in the diaphragmatic contour by the herniated retroperitoneal fat.

Fig 3: HYPOGENETIC LUNG SYNDROME





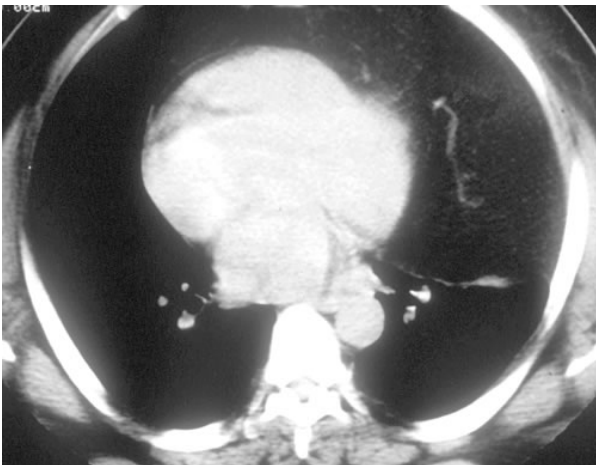
Right paracardiac mass incidentally discovered on routine chest radiography in an asymptomatic 45-year-old man. A. Chest radiograph: small right lung with anomalous venous return (small arrows) and round regular opacity in the right lower hemithorax (arrows) suggestive of pulmonary sequestration. B. CT scan with pulmonary window setting: anomalous venous return of right inferior pulmonary vein (arrows) to the inferior

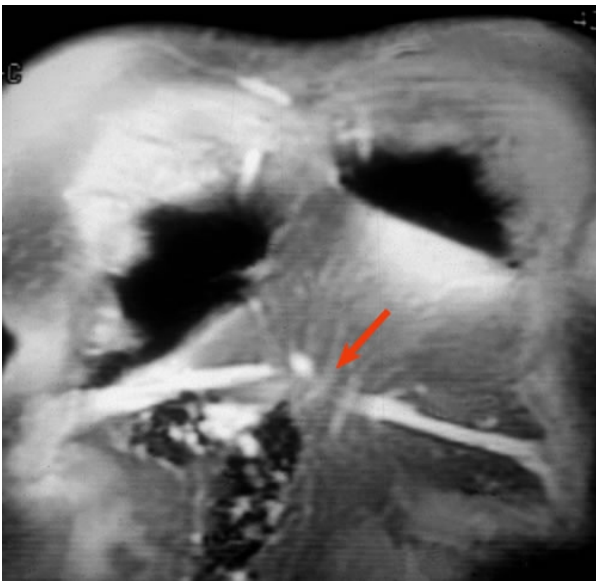
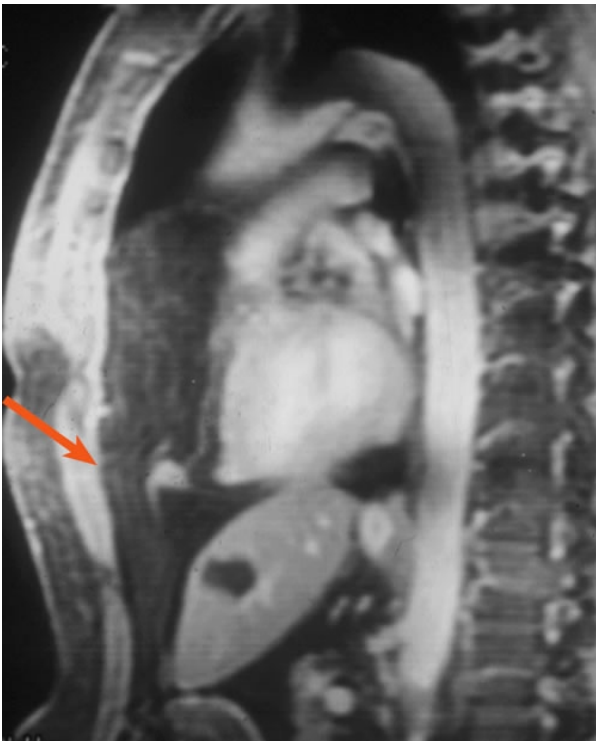
vena cava. C. Contrast-enhanced CT scan: a portion of liver herniated into the chest (arrow). D. Coronal contrast-enhanced MRI: Bochdalek hernia with herniated liver and anomalous venous return (arrow). E. MRI angiography: anomalous venous return (white arrows) and Budd-Chiari syndrome (arrows) due to liver hernia compressing hepatic veins.

Morgagni Hernia

Anterior hernias of the foramina of Morgagni are very rare, result from failure of fusion of the septum transversum with the body wall, and usually present later in life. Morgagni hernias are most often in the right side, because left herniation is prevented by the heart and pericardium. These hernias are mostly asymptomatic, although lower sternal discomfort, cough, dyspnea and non-specific gastrointestinal symptoms may occur. Imaging features vary depending on the herniated contents that include omentum, liver, or colon. On chest radiography, they typically appear as a well-defined opacity in the right cardiophrenic angle. Air-containing loops of small or large bowel are occasionally seen. The diagnosis of Morgagni hernia can be readily made on CT or MRI (Fig).

Fig: MORGAGNI HERNIA



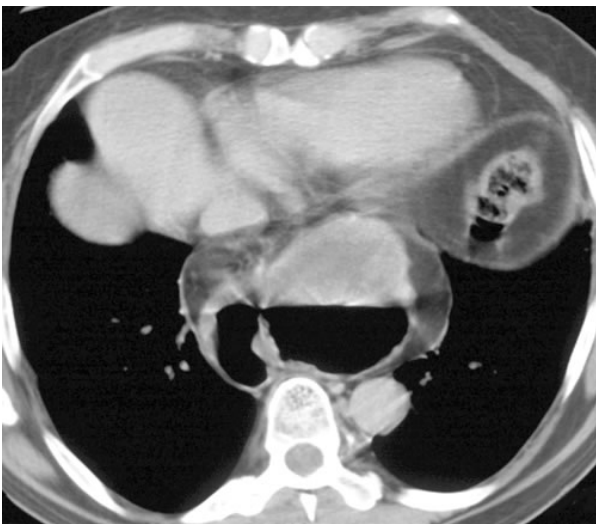


An asymptomatic 35-year-old man A. Routine chest radiograph: homogeneous regular mass obscuring right and left cardiophrenic angle mimicking cardiomegaly. B. CT scan: huge fatty density mass containing vascular structures in the left lower chest and precardiac area. C. Sagittal and D. Coronal contrast-enhanced T1-weighted MRI with fat suppression: small defect (arrows) of the anterior part of the diaphragm with herniated omental fat.

hiatal hernia

A hiatal hernia results from the extension of the stomach into the chest through the esophageal hiatus. Acquired enlargement of the esophageal hiatus and laxity of the phrenoesophageal ligament are causative factors, often associated with obesity or pregnancy. Hiatal hernia are frequent incidental findings on chest radiographs and CT. On chest radiography, they typically appear as round retrocardiac masses, usually containing air or an air-fluid level. The diagnosis is easily confirmed by a barium esophagogram or CT. CT scans reveal extension of a portion of the proximal stomach into the lower mediastinum, and an abnormally wide esophageal hiatus (Fig).

Fig: HIATAL HERNIA



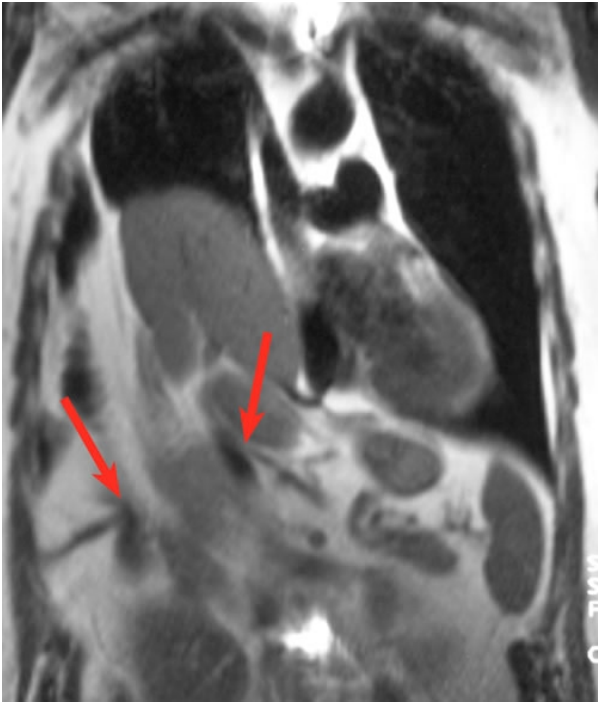
Follow-up of breast cancer in an asymptomatic 56-year-old woman. A. Chest radiograph: large retrocardiac mass containing air. B. CT scan: dilated stomach with air-fluid level in the retrocardiac area. CT was performed in prone position for the lung nodule biopsy.

traumatic hernia

Traumatic diaphragmatic hernia can result from either penetrating or blunt injury. Diaphragmatic rupture is associated with severe injury and a high mortality secondary to the associated injuries. Diaphragmatic rupture occurs in 0.8% to 8% of patients after blunt trauma. It usually affects the left side. Diagnosis of the diaphragmatic rupture is often missed but the lesion is more readily recognized if the injury is recent and the tear is large and left-sided. Diagnostic radiographic signs of diaphragmatic rupture include visualization of herniated stomach or bowel in the chest and cephalad extension of an intragastric tube above the level of the diaphragm. Suggestive findings include irregularity of the diaphragmatic contour, elevated hemidiaphragm in the absence of the atelectasis, and a contralateral shift of the mediastinum in the absence of the pleural effusion or pneumothorax. Characteristic CT findings of diaphragmatic tear include sharp discontinuity of the diaphragm, intrathoracic visceral herniation, lack of visualization of a hemidiaphragm (absent diaphragm sign), and constriction of bowel or stomach at the site of herniation (collar or waist sign). Although retrospective analysis indicates that most diaphragmatic tears are detectable by CT, several studies have found CT to be of limited value in diagnosis. In problematic cases, coronal and sagittal MR imaging or spiral CT with multiplaner reconstruction can be definitive. These imaging planes can be useful in depicting the secondary sign of focal bulge or mushrooming in the diaphragmatic contour, particularly on the right where diagnosis can be difficult. MRI has the advantage of being capable of identifying the entire diaphragm as a distinct and separate structure, whereas, CT is limited in this regard.

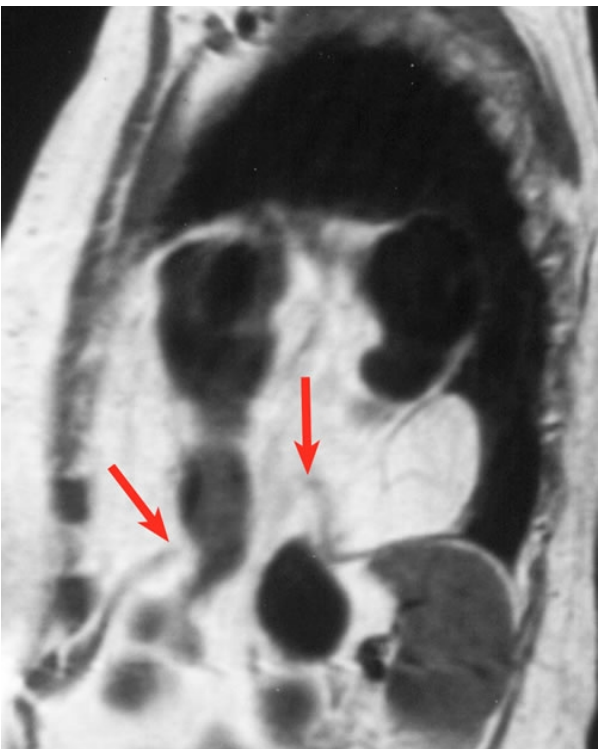
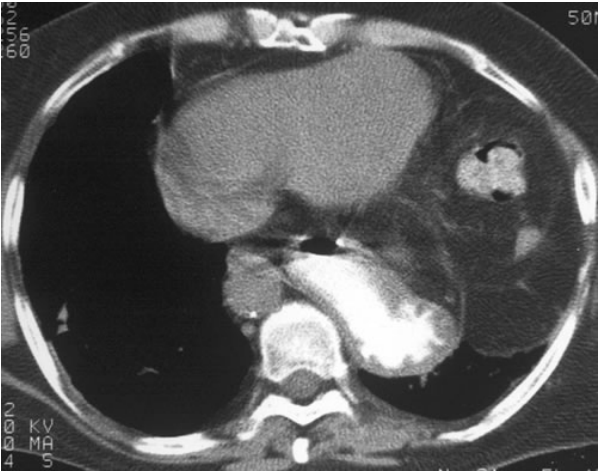
Fig 1: TRAUMATIC DIAPHRAGMATIC HERNIA





A 66-year-old man with previous history of car accident 13 years ago complained of increasing shortness of breath. A. Chest radiograph: apparent elevation of the right hemidiaphragm. B. Coronal T1-weighted MRI: discontinuity of the right diaphragm (black arrows) and bowel herniation. C. Barium enema and UGI: herniation of the colon and a portion of stomach through the tear.

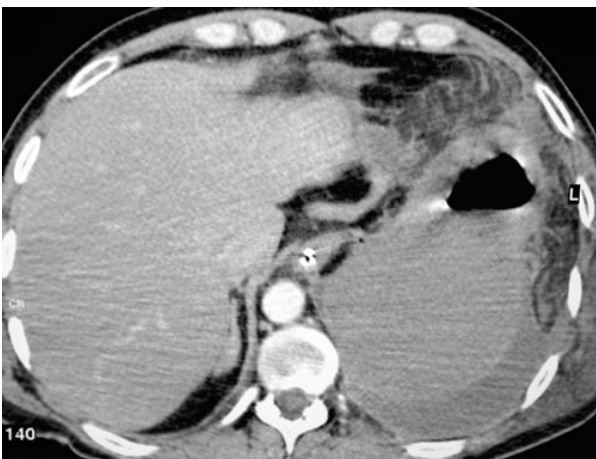
Fig 2: RUPTURED DIAPHRAGM WITH CONGENITAL HIATAL HERNIA

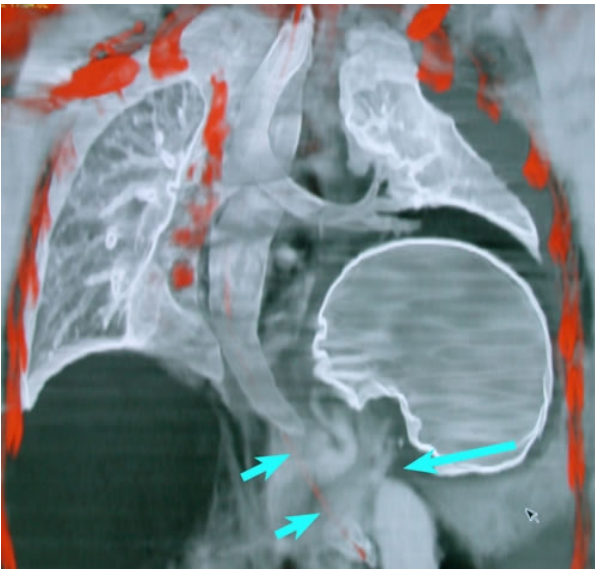
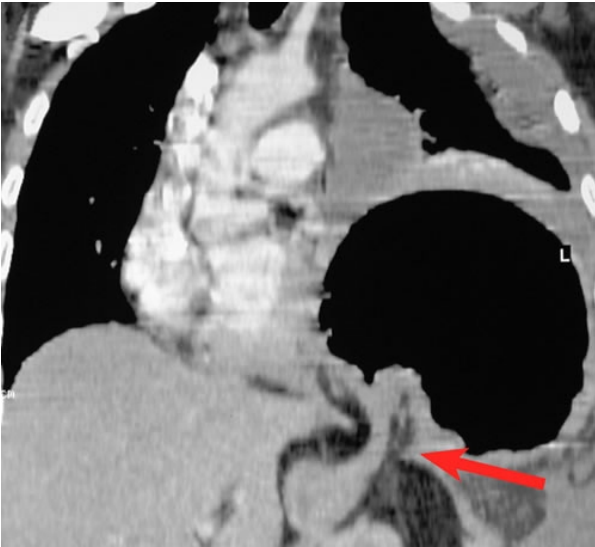




A 59-year-old woman complained of exertional dyspnea since 3 years. She was involved in automobile accident 17 years previously. A. Radiograph: Numerous air-containing viscera within the lower portion of the left hemithorax. Note the old tuberculous lesion of the right lung and pleura. B. CT scan through the lower chest: herniation of a portion of the stomach in to the lower mediastinum and abnormally high position of the colon. C. Sagittal T1-weighted MRI: free edge of the torn left diaphragm (arrows) with herniated colon through the orifice of 5 cm in diameter. D. Coronal T1-weighted MRI: herniated stomach through the esophageal hiatus covered by hernial sac (small arrows). Sugery confirmed the diaphragmatic tear located just lateral to the esophageal hiatus.

Fig 3: TRAUMATIC DIAPHRAGMATIC HERNIA





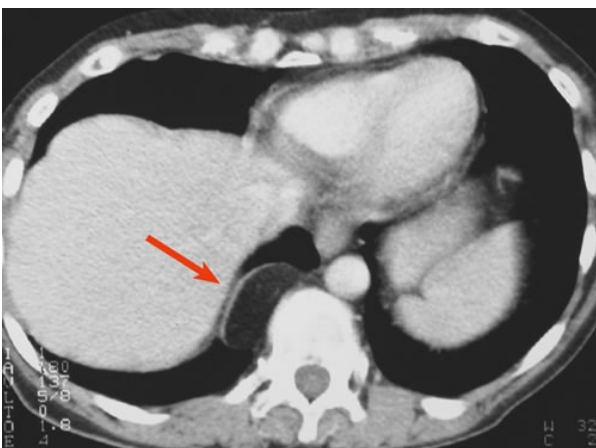
A 35-year-old man with previous history of aortic surgery for isthmic pseudoaneurysm after a car accident 2 years ago complained of severe chest pain and dyspnea for 3 days. Chest radiograph at emergency room shows an opacification of the left hemithorax. A. Contrast-enhanced multi-detector row CT scan: lack of visualization of the left hemidiaphragm and dependant viscera sign. B. Sagittal and C. Coronal reformatted image: severe constriction of the stomach at the site of herniation (collar sign). D. Coronal volume-rendered CT image shows well the herniated constricted stomach (long arrow), dilated esophagus, and pleural effusion and collapsed left lung. Note also the normal position of the nasogastric tube (small arrows) in the non herniated portion of the stomach. At surgery, gastric strangulation was found.

8) Tumors of the diaphragm

Primary tumors of the diaphragm are very rare. Benign tumors are most common, with lipomas and cystic masses such as bronchogenic and mesothelial cyst. Other benign tumors include hemangioma, angiofibroma, neurofibroma, schwannoma, leiomyoma, teratoma, endometrioma, and desmoid tumor. Most malignant tumors are sarcomas of fibrous or muscular origine. They include fibrosarcoma, malignant fibrous histiocytoma, hemangiopericytoma, germ cell tumors, pheochromocytoma, and leiomyosarcoma. Radiologically, most diaphragmatic tumors present as smooth or lobulated soft-tissue masses protruding into the inferior portion of the lung or can resemble a diaphragmatic hernia, eventration or plural lesion. CT or MR imaging can easily confirm the presence of a mass in the diaphragm. When the tumor is large, it may not be possible to determine whether it arise from diaphragm, pleura, or lungs, or abdominal viscera, even on CT, MR imaging, or ultrasound. Thoracic or abdominal tumors may secondarily involve the diaphragm by direct extension. Such tumors include bronchogenic carcinoma, mesothelioma, and other primary or secondary pleural or chest wall malignancies, hepatic neoplasms, and peritoneal carcinomatosis. Diaphragmatic metastases, derived from either lymphatic or hematogenous spread, are rare. Clinical symptoms or radiographic features are usually related to the presence of neoplasm in contiguous structures or elsewhere, rather than in the diaphragm itself.

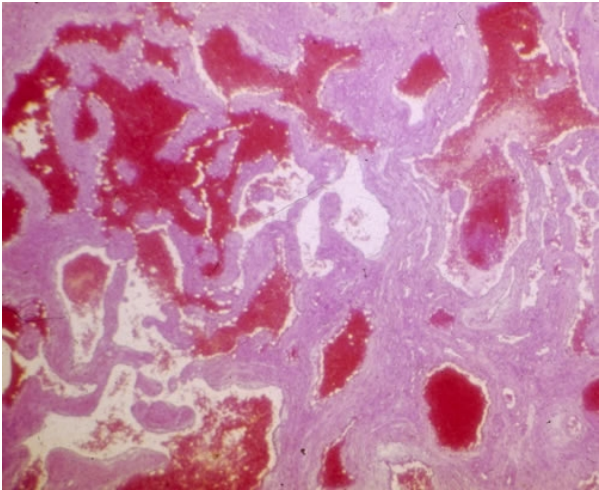
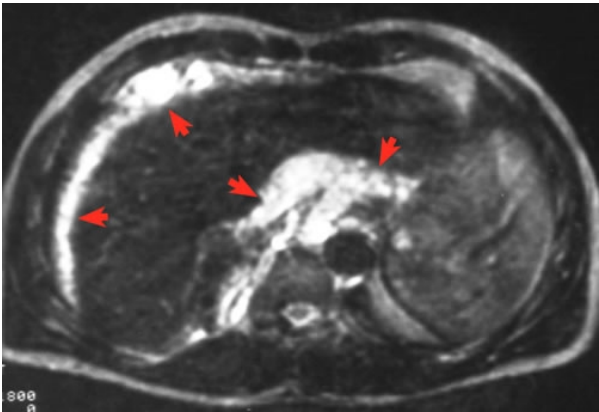
Lipoma

LIPOMA



An asymptomatic 64-year-old woman. CT shows a low-attenuation mass (arrow) in the crus of the right diaphragm.

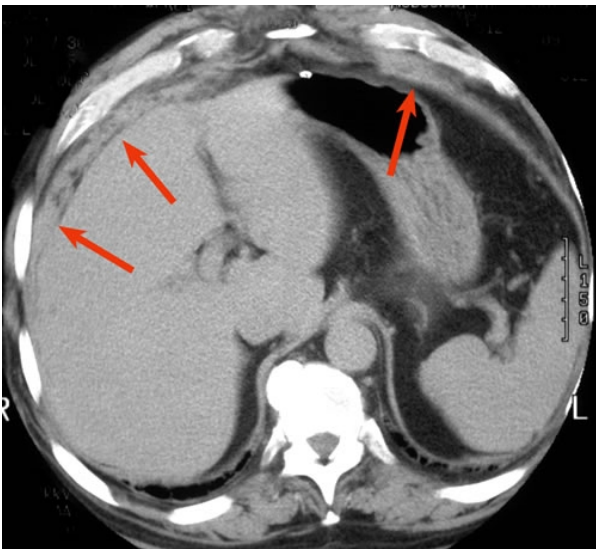
hemangioma



HEMANGIOMA

A 42-year-old man with intermittent abdominal pain. A. Contrast-enhanced CT: diffuse irregular thickening of the right hemidiaphragm (small arrows) and low density nodules in the spleen. Note also multiple phleboliths (long arrows) in the tumor. B. T2-weighted MRI: extremely high-signal intensity of the right diaphragm and the coeliac area. Splenic nodules have same signal intensity as the diaphragmatic lesion. C. Photomicrograph of surgical biopsy specimen (x25, H-E stain): numerous vascular spaces of irregular size separated by fibrous trabeculae.

histiocytoma

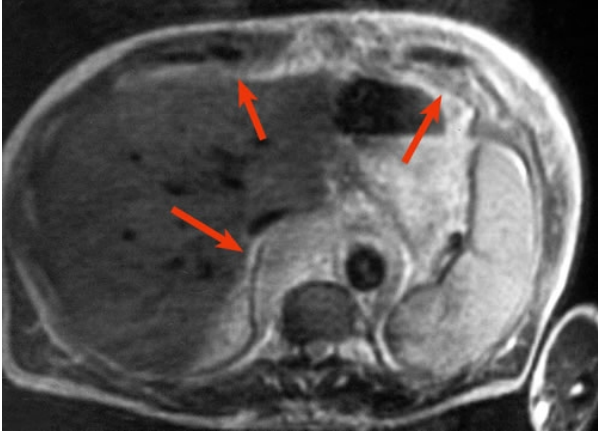


MALIGNANT FIBROUS HISTIOCYTOMA

A 73-year-old man with vague thoracic pain. CT scan shows diffuse irregular thickening of the anterior part of the diaphragm.

Lymphoma



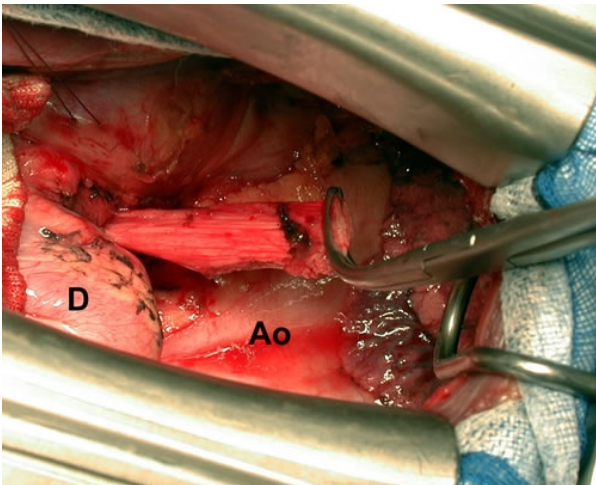
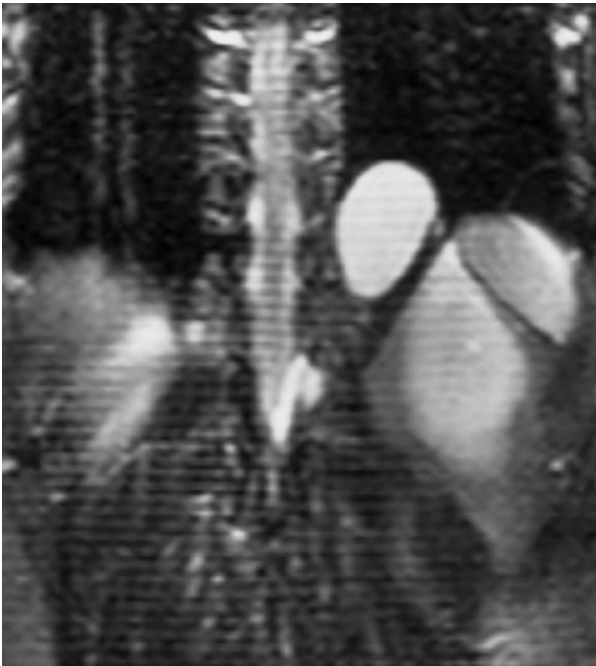


LYMPHOMA

A 62-year-old man with a lower thoracic wall mass and a 3-month history of vague discomfort. A. Contrast-enhanced CT scan demonstrates diffuse thickening of the thoracic wall, left diaphragm and right crus (arrows). B. T2-weighted MRI: moderately high-signal intensity infiltrating tumor.

bronchogenic cyst

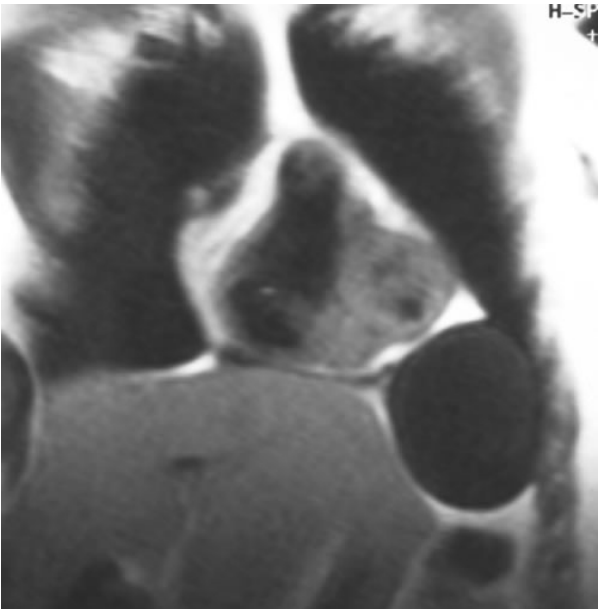




DIAPHRAGMATIC BRONCHOGENIC CYST

A 45-year-old man with back pain for 2 years. A. Non-enhanced CT: high-density ovoid mass within the left crus of diaphragm. B. Coronal T2-weighted fat suppressed MRI: very high-signal intensity ovoid cyst in the diaphragm. C. Surgery: extraction of the collapsed bronchogenic cyst after simple diaphragmatic incision. The diaphragm (D) is seen on the left, and aorta (Ao) at the bottom.

pleuropericardial cyst

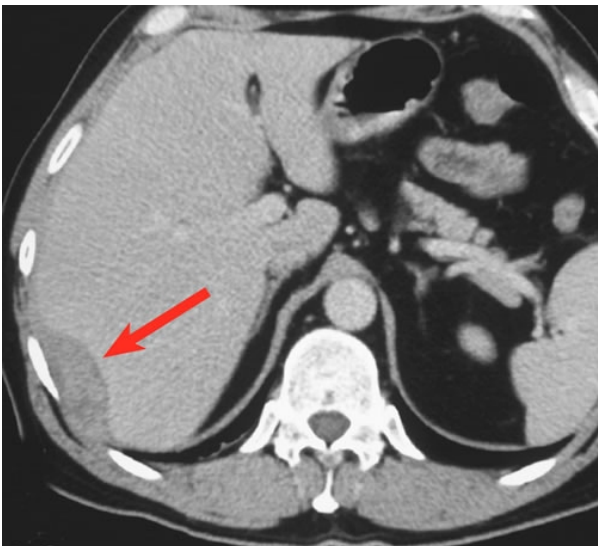


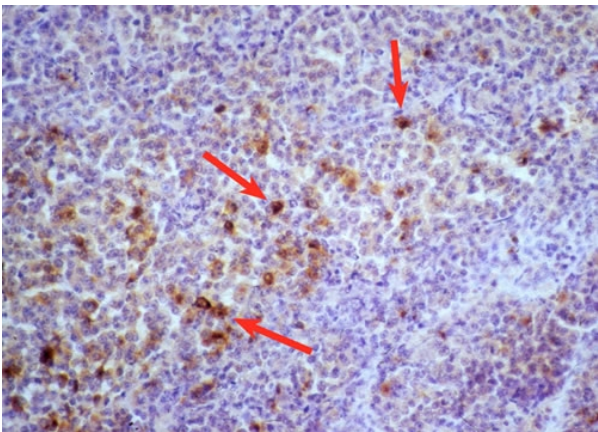
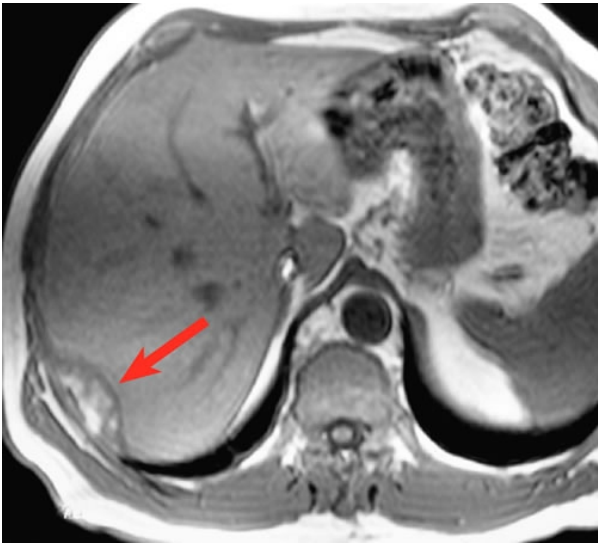


DIAPHRAGMATIC PLEUROPERICARDIAL (MESOTHELIAL) CYST

A 56-year-old woman with a 4-year-history of epigastric pain. A. Chest radiograph: round homogenous opacity in the left cardiophrenic angle. B. Contrast-enhanced CTscan: water-density mass anterior to the left lobe of the liver. C. coronal T1-weighted MRI: low-signal intensity mass within the anterior part of the diaphragm. D. Coronal T2-weighted MRI: homogenous high-signal intensity thin-walled cyst.

Metastases



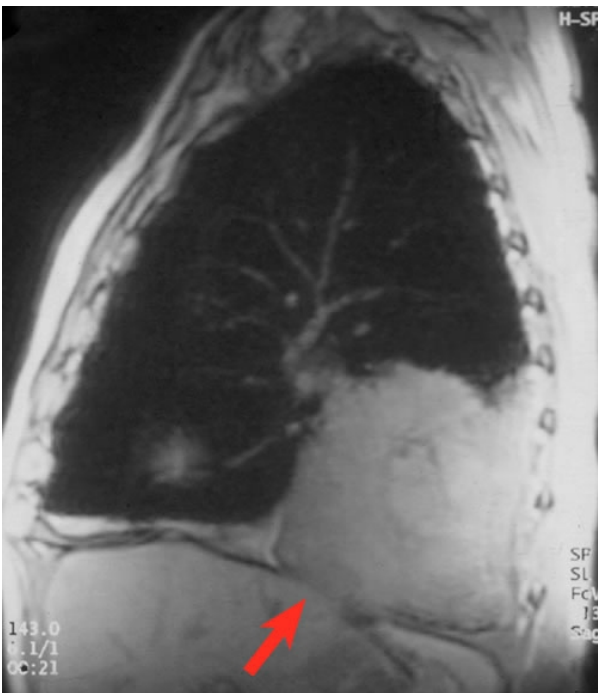


METASTASES

DIAPHRAGMATIC METASTASIS OF MELANOMA

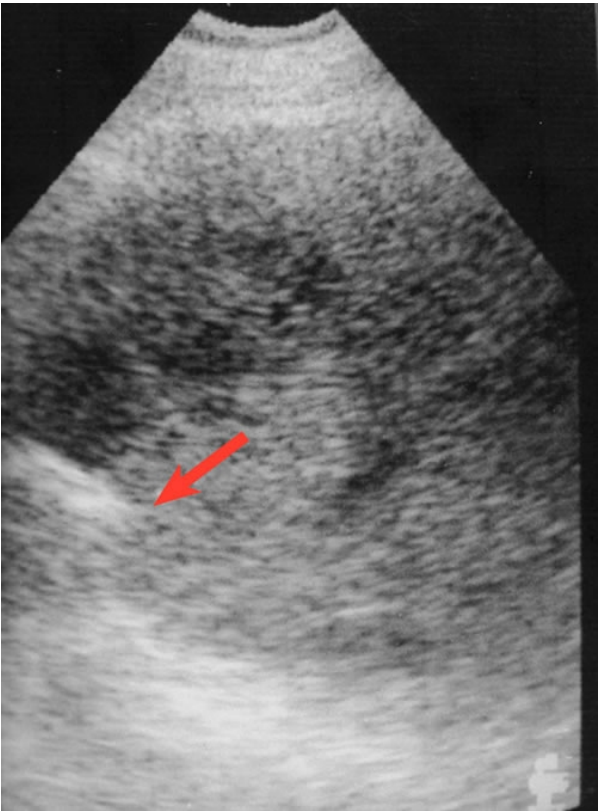
A 57-year-old man with tumor recurrence at the scar of previous resection of left anterior chest wall melanoma 7 years before. A. Contrast-enhanced CT scan: low density ovoid mass in the right diaphragm compressing the hepatic parenchyma. B. T1-weighted MRI: heterogeneous tumor with high-signal intensity areas due to the presence of paramagnetic melanin. Needle biopsy confirmed the melanoma. C. Photomicrograph of needle biopsy specimen (x50, HMB 45 stain): multiple melanin pigment containing cells (arrows).

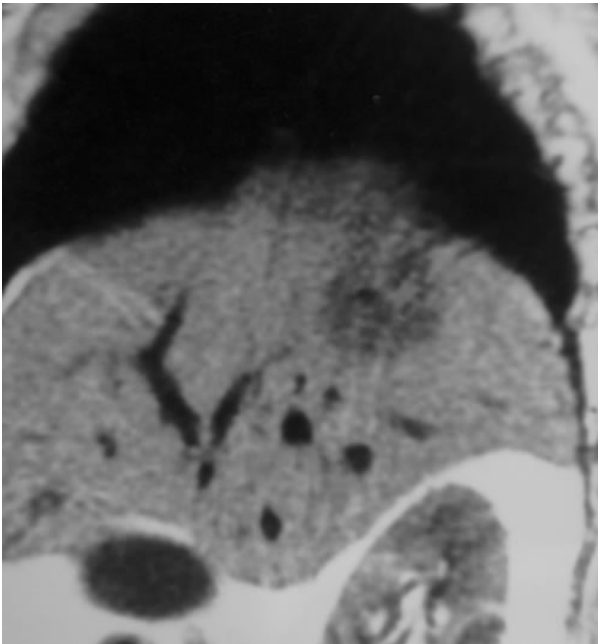
BRONCHOGENIC CARCINOMA



T1-weighted MRI shows a diaphragmatic invasion (arrow) by the right lower lobe tumor in a 45 year-old man.

DIAPHRAGMATIC METASTASIS OF THE PHARYNGEAL CARCINOMA





A 60-year-old man with a history of pharyngeal carcinoma treated 2 years before. A. Follow-up chest radiograph: round opacity in the right peridiaphragmatic area. B. Longitudinal sonogram: disruption of the diaphragm (arrows) by slightly hyperechoic irregular hepatic nodule. C. Sagittal T1-weighted MRI: low-signal intensity dumbbell-shaped mass located in the diaphragm and the liver.

9) REFERENCES

1. Alexander C. Diaphragm movements and the diagnosis of diaphragmatic paralysis. *Clin Radiol* 1966; 17: 79-83.
2. Brink JA, Heiken JP, Semenkovich J, et al. Abnormalities of the diaphragm and adjacent structure: Findings on multiplaner spiral CT scans. *AJR* 1994; 163: 307-310.
3. Buetow PC, Kransdorf MJ, Moser RP Jr, Jelinek JS, Berry BH. Radiologic appearance of intramuscular hemangioma with emphasis on MR imaging. *AJR* 1990; 154: 563.
4. Caskey CI, Zerhouni EA, Fishman EK, Rahmouni AD. Aging of the diaphragm: a CT study. *Radiology* 1989; 171: 385-389.
5. Currarino G, Williams B. Causes of congenital unilateral pulmonary hypoplasia: a study of 33 cases. *Pediatr Radiol* 1985; 15: 15-24.
6. Dee P. Congenital disorders of the lungs and airways. In: Armstrong P, Wilson AG, Dee P, Hansell DM, eds. *Imaging of diseases of the chest*, 3rd ed.; London, Mosby, 2000; 689-725.
7. Deslauriers J. Eventration of the diaphragm. *Chest Surg Clin North Am* 1998; 8: 315-330.
8. Dosios T, Papachristos IC, Crisicopoulos H. magnetic resonance imaging of blunt traumatic rupture of right hemidiaphragm. *Eur J Cardiothorac Surg* 1993; 7: 553-554.
9. Fraser RG, Paré JAP, Paré PD, Fraser RS, Genereux GP. Diseases of the diaphragm and chest wall. In: Fraser RG, Paré JAP, Paré PD, Fraser RS, Genereux GP, eds. *Diagnosis of diseases of the chest*, 3rd ed.; Philadelphia, Saunders WB Company, 1991; 2921-2973.
10. Gale ME. Bochdalek hernia; Prevalence and CT characteristics. *Radiology* 1986; 156: 449-452.
11. Gierada D, Slone RM, Fleishman MJ. Imaging evaluation of the diaphragm. *Chest Surg Clin North Am* 1998; 8: 237-280.
12. Heitzman ER. Kerly Pergamon lecture: The diaphragm. Radiologic correlations with anatomy and pathology. *Clin Radiol* 1990; 42: 15-19.
13. Kuhlman JE, Pozniak MA, Collins J, Knisely BL. Radiographic and CT findings of blunt chest trauma: Aortic injuries and looking beyond them. *RadioGraphics* 1998; 18: 1085-1106.
14. Langer JC. Congenital diaphragmatic hernia. *Chest Surg Clin North Am* 1998; 8: 295-314.
15. Laxdal OE, McDougall H, Mellin GW. Congenital eventration of the diaphragm. *N Engl J Med* 1954; 250: 401-408.
16. Müller NL, Fraser RS, Colman NC, Paré PD. Disease of the diaphragm and chest wall. In: Müller NL, Fraser RS, Colman NC, Paré PD, eds. *Radiologic diagnosis of the diseases of the chest*. Philadelphia, Saunders WB Company, 2001; 749-768.
17. McHugh K, Ogilvie C, Brunton FJ. Delayed presentation of traumatic diaphragmatic hernia. *Clin Radiol* 1991; 43: 246-250.
18. Naidich DP, Megibow AJ, Ross CR, Beranbaum ER, Sigelman SS. Computed tomography of the diaphragm: Normal anatomy and variants. *J Comput Assist Tomogr* 1983; 7: 633-640.
19. Naunheim KS. Adult presentation of unusual diaphragmatic hernias. *Chest Surg Clin North Am* 1998; 8: 359-369.

20. Patridge JB, Osborne JM, Slaughter RE. Scimitar etcetera: the dysmorphic right lung. *Clin Radiol* 1988; 39: 11-19.
21. Press GA, Glazer HS, Wasserman TH et al. Thoracic wall involvement by Hodgkin disease and non-Hodgkin lymphoma: CT evaluation. *Radiology* 1985; 5: 195.
22. Silverman PM, Godwin JD, Korobkin M. Computed tomographic detection of retrocrural air. *AJR* 1982; 138: 825-827.
23. Tarver RD, Conces DJJ, Cory DA, et al. Imaging of the diaphragm and its disorders. *J Thorac Imaging* 1989; 4: 1-18.
24. Worthy SA, Kang EY, Hartman TE, et al. Diaphragmatic rupture: CT findings in 11 patients. *Radiology* 1995; 194: 885-888.
25. Shanmuganathan K, Mirvis SE, White CS, et al. MR imaging of the hemidiaphragms in acute blunt trauma: experience with 16 patients. *AJR* 1996; 167: 397-402.
26. Weksler B, Ginsberg RJ. Tumors of the diaphragm. *Chest Surg Clin North Am* 1998; 8: 441-447.